

Performance of ammonia water absorption machine

Abir HMIDA*, Nihel CHEKIR², Mouna HAMED³, Ammar BEN BRAHIM⁴

^{1,2,3,4}R.U. Applied Thermodynamic, National Engineering School of Gabes, Gabes University, Omar IbnElkhatib Street, Zrig, 6072 Gabes Tunisia

E-mail: ¹hmida.abir1@gmail.com, ²nihel.chekir@yahoo.fr, ³hamedm@hotmail.fr, ⁴ammar.benbrahim@enig.rnu.tn

(*: Corresponding Author)

Abstract: we provide in this paper an absorption chiller destined for cooling storage food (in cold room of 45 m³) in the south of Tunisia. An overview of these machines and working fluids are presented. In addition, a thermodynamic study and simulation results, carried out using Matlab Software, were established for the absorption refrigerator.

Keywords: Refrigeration – Ammonia – Gibbs Energy – Matlab.

I. INTRODUCTION

The agriculture field in Tunisia suffers from problem of storage of natural products especially fruits and vegetables. Tons of products are usually rotten and lost because of lack of preservation methods such as refrigeration. Food refrigeration offers slow growth of bacteria and preserves fibers, which makes its life longer and keeps the maximum of their minerals and vitamins.

In recent years, special attention has been paid to absorption systems [1]. These refrigeration systems are considered an alternative solution to improve the agricultural field particularly in the south of Tunisia since it can be driven by low temperature sources and characterized by the environmentally friendly operation and a low total cost [2].

II. LITERATURE REVIEW

The early development of an absorption cycle dates back to the 1700's by Nairn [3], using stored ice and a number of evaporative process, but the first commercial refrigerator was only built and patented by Ferdinand Carré in 1823 [4]. Using water/ammonia as a working fluid, he introduced a novel machine by the year 1859 [3], which were used to make ice and store food. This system went through difficulties, being the antecessor of the vapor compression refrigeration system in the 19th century. With ammonia–water as working fluid, machines found wide application in residential and industrial refrigerators [4]. In the 1940's, lithium bromide/water system was introduced and by 1950 it was commercialized for an independent industrial applications. Research and developments were carried

out and few years later, the double effect system was introduced and used as an industrial standard for a high performance heat-operated absorption cycle [3].

In the 1970's the substitution to petroleum-based combustion fuels affected the application of absorption refrigeration, but, in the other hand, new opportunities arose, such as usage of solar energy to drive this system [4].

III. WORKING FLUID

Unlike theoretical performances, the real performance of absorption refrigeration machines depends on the nature of the refrigerant used. The search for efficient refrigerants for these machines is of great importance [5]. Since the 1930s, Chlorofluorocarbons and Hydrochlorofluorocarbons (CFCs and HCFCs) have been widely used as refrigerant in air conditioning and refrigeration system [6] due to their favorable characteristics. As Refrigerant R-12 was the most dominant and developed in the refrigeration industry since it is inexpensive, nonflammable and very stable [7]. CFC's were used for domestic refrigerators and small refrigeration units. Unfortunately, CFCs were found to be the main cause of ozone layer depletion and make a significant contribution to global warming when emitted to atmosphere [6]. The discovery of the ozone hole over the Antarctic led to the Montreal Protocol in 1989. Therefore, CFCs had to be regulated and prohibited from the refrigeration industry. It was proposed to be phased out by the year 1996 in developed countries, and 2010 for developing countries. The deadline for the phase out of R22, according to Kyoto Protocol in 1997, is 2020 in developed countries and 2030 for the developing countries [8].

The issue of CFCs was a 'hot' topic for researchers and manufacturers in refrigeration and air conditioning fields because of their impact of the ozone. Studies on manufacturing plants operating with 'ozone safe' substances were carried out to find a satisfactory solution to the problem.

The refrigerant must be safe both to the environment and to human. At the same time, it must present suitable thermodynamic parameter such as the condensing pressure, pressure ratio, latent enthalpy and the isentropic exponent. It must also have no chemical reactions when it comes into contact with metals, polymers or lubricating oils [9]. Finally, it must be stable at high temperatures, non-flammable, non-explosive[10], zero ozone layer depletion and easily available at low cost and the elevation of boiling should be as large as possible [11], Dongsoo Jung presents some of refrigerant properties [13].

Despite of the research efforts, only two mixtures remain almost exclusively used: aqueous solutions of lithium bromide and ammonia. However, an installation operating with an aqueous solution of lithium bromide cannot produce cold at temperatures below 0 ° C. With a high salt content, the risk of crystallization is high [5]. The water–ammonia mixture is used in many industrial processes. Its thermal properties makes it the most important refrigerants in the absorption refrigerating and climatic applications. For a reliable design of an absorption refrigeration machines a reliable prediction of refrigerant mixture thermodynamic properties is required. Power cycle Kalina's proposition in 1983 has led to a significant increasing of the research effort on the ammonia–water mixture properties. The availability of new databank has allowed the formulation of unified empirical equations based on Gibbs free energies [12].

IV. ABSORPTION REFRIGERATION SYSTEM

Between 1970 and 2004 and according to the Intergovernmental Panel on Climate Change (IPCC), Global Greenhouse Gas emission (GHG) has increased by 70%, growing from 28.7 to 49 GtCO_{2-eq} (Gigatonnes of carbon dioxide equivalent). A report from the International Energy Agency illustrated that 65% of greenhouse gas emissions in 2009 were related to energy use of some kind. As an example, a 16% from the building sector, 25% from the power generation sector and other emissions sources reductions are needed. Therefore, steps toward climate change must focus on decarbonizing energy technologies. Environmentally friendly and energy-efficient technologies must be upgraded so that the environmental impact of the cooling and heating needs in the building sector is minimized with low cost. [14]

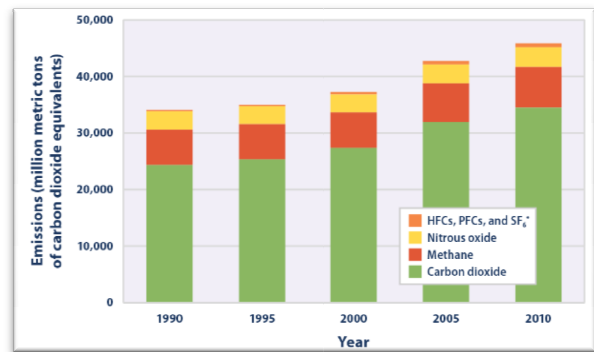


Figure 1: Global Greenhouse Emissions by Gas 1990-2010

Because of their benefits to both the environment and energy consumption, absorption cycles are gaining popularity in air conditioning and refrigeration systems. In comparison with vapor compression cooling cycles the main advantage of heat-driven chillers is their capability to use a low-grade energy available from solar, geothermal, biomass as well as from waste heat recovered from thermal systems. Moreover, refrigerant in absorption systems have zero global warming potential and do not contribute to ozone layer depletion [14]

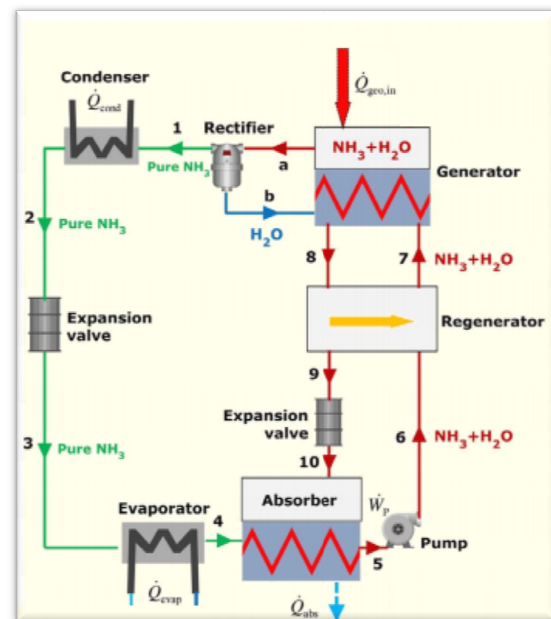


Figure 2: Absorption Refrigeration Machine

Heat is provided to ammonia/water solution contained in the generator, producing ammonia evaporation, which leaves the mixture. The produced steam flows to the condenser [2] where it liquefies by releasing heat. The generator-condenser unit constitutes the high-pressure part of the system as illustrated in (fig.2) [15]

Liquid refrigerant getting out from the condenser can then be expanded from this high-pressure zone to the low-pressure evaporator.

The energy required for vaporization is borrowed from fluid circulating in the evaporator which will, of course, be cooled. After refrigerant evaporation in the evaporator and heat extraction from the environment to be cooled, the refrigerant afterward directed to the absorber [2]; therein, the solution with low concentration of ammonia absorbs the refrigerant [1]. Since this recombination is exothermic, it is necessary to extract heat from the absorber to maintain its temperature low enough to keep the high affinity needed between the refrigerant and the solution. The resultant rich solution is collected at the bottom of the absorber and re-pumped into the generator. It is the circulation pump which ensures the desired difference pressure in the system. The need to circulate continuously, in one hand, poor refrigerant solution from the high temperature generator to a low temperature absorber and on the other hand the refrigerant-rich solution counter-currently suggests the installation of a heat recuperator[16]. A simple, systematic heat exchanger that minimizes heat losses associated to fluid transfers between the two components, which increases the coefficient of performance COP [17]. In the recuperator absence, the thermal load on the heat source and the thermal rejection associated with the absorber would be increased, leading to performance coefficient's decrease.

V. MODELISATION

The operating parameters of an absorption machine are closely related. The change of a parameter causes the variation of all the others. When an input variable changes, the entire cycle reacts to establish a new equilibrium state. This dynamic nature of the absorption cycle operating equilibrium states must be taken into account when studying the cycle [18]. Each component of the chiller is controlled by mass and energy balance.

A. Mass balance

$$\dot{m} + \dot{p} - \dot{r} = 0 \quad (1)$$

$$\dot{m} + x_p \dot{p} - x_r \dot{r} = 0 \quad (2)$$

$$\dot{r} = m \frac{1 - x_p}{x_r - x_p} \quad (3)$$

$$\dot{p} = m \frac{1 - x_r}{x_r - x_p} \quad (4)$$

x_r : Poor solution title of ammonia leaving the generator to the absorber.

x_p : Ammonia title in rich mixture leaving the absorber to the generator.

B. Enthalpy balance

$$\dot{Q}_a + \dot{Q}_c = \dot{Q}_e + \dot{Q}_g + W \quad (5)$$

- In the generator:

$$\dot{Q}_g = \dot{m} h_a + \dot{p} h_8 - \dot{r} h_7 \quad (6)$$

- In the evaporator:

$$\dot{Q}_e = \dot{m} (h_4 - h_3) \quad (7)$$

- In the absorber:

$$\dot{Q}_a = \dot{p} h_{10} + \dot{r} h_5 - \dot{m} h_4 \quad (8)$$

- In the condenser

$$\dot{Q}_c = \dot{m} (h_2 - h_1) \quad (9)$$

- In the pump:

$$W = \dot{r} (h_6 - h_5) = V (P_6 - P_5) \quad (10)$$

- Solution specific flow:

$$f = \frac{\dot{r}}{\dot{m}} = \frac{1 - x_p}{x_r - x_p} \quad (11)$$

- Performance coefficient:

$$COP = \frac{\dot{Q}_c}{\dot{Q}_g - W} \quad (12)$$

VI. THERMODYNAMIC MODELING OF (NH₃/H₂O) PROPERTIES

A. Pure components

In this study, the Gibbs energy is used for the calculation of pure ammonia and water thermodynamic properties as well as the ammonia-water mixture. The fundamental equation of Gibbs free enthalpy is given in an integral form [20]

$$G = H_0 - TS_0 + \int_{T_0}^T c_p dT + \int_{T_0}^T V dP - T \int_{T_0}^T \frac{c_p}{T} dT \quad (13)$$

The behavior of the liquid state from the thermal point of view is described by the following correlations; where the volume is a function of the pressure and the temperature.

$$V^L = a_1 + a_2 P + a_3 T + a_4 T^2 \quad (14)$$

$$c_p^L = b_1 + b_2 T + b_3 T^2 \quad (15)$$

$$V^g = \frac{RT}{P} + C_1 + \frac{C_2}{T^3} + \frac{C_3}{T^{11}} + \frac{P^2 C_4}{T^{11}} \quad (16)$$

$$c_p^g = d_1 + d_2 T + d_3 T^2 - T \int_{P_0}^P \left(\frac{\partial^2 V}{\partial T^2} \right) dP \quad (17)$$

The following reduced form is obtained by the development of the equation 13

a. Liquid phase

$$\begin{aligned} G_r^l &= H_{r,0}^l - T_r S_{r,0}^l + B_1 (T_r - T_{r,0}) + \\ &\frac{B_2}{2} (T_r^2 - T_{r,0}^2) + \frac{B_3}{3} (T_r^3 - T_{r,0}^3) - B_1 T_r \ln \left(\frac{T_r}{T_{r,0}} \right) \\ &- B_2 T_r (T_r - T_{r,0}) - \frac{B_2}{2} T_r (T_r^2 - T_{r,0}^2) + \\ &\left(A_1 + A_3 T_r + A_4 T_r^2 \right) (P_r - P_{r,0}) + \frac{A_2}{2} (P_r^2 - P_{r,0}^2) \end{aligned} \quad (18)$$

b. Vapor phase

$$\begin{aligned} G_r^g &= H_{r,0}^g - T_r S_{r,0}^g + D_1 (T_r - T_{r,0}) + \frac{D_2}{2} (T_r^2 - T_{r,0}^2) \\ &+ \frac{D_3}{3} (T_r^3 - T_{r,0}^3) - D_1 T_r \ln \left(\frac{T_r}{T_{r,0}} \right) - D_2 T_r (T_r - T_{r,0}) \\ &- \frac{D_3}{2} T_r (T_r^2 + T_{r,0}^2) + T_r \ln \left(\frac{P_r}{P_{r,0}} \right) + C_1 (P_r - P_{r,0}) \\ &+ C_2 \left[\frac{P_r}{P_{r,0}^3} - 4 \frac{P_{r,0}}{P_{r,0}^3} + 3 \frac{T_r P_{r,0}}{T_{r,0}^4} \right] + C_3 \left[\frac{P_r}{T_r^{11}} - 12 \frac{P_{r,0}}{T_{r,0}^{11}} + 11 \frac{T_r P_{r,0}}{T_{r,0}^{12}} \right] \\ &+ \frac{C_4}{3} \left[\frac{P_r}{T_r^{11}} - 12 \frac{P_{r,0}}{T_{r,0}^{11}} + 11 \frac{T_r P_{r,0}}{T_{r,0}^{12}} \right] \end{aligned} \quad (19)$$

Dimensionless quantities are:

Reduced temperature: $Tr = T/T_B$;

Reduced molar free enthalpy: $Gr = G/RT_B$;

Reduced pressure: $Pr = P/P_B$;

Reduced molar enthalpy: $Hr = H/RT_B$;

Reduced molar entropy: $Sr = S/R$;

Reduced molar volume: $Vr = VP_B/RT_B$.

Where $T_B = 100K$, $P_B = 10bar$ and

$R = 8.3143KJ/Kmole.K$.

This equation is valid for the gaseous phase, as well as liquid one. Enthalpy, entropy and molar volume are related to the Gibbs energy:

$$H = -RT_B T_r^2 \left[\frac{d \left(\frac{G_r}{T_r} \right)}{dT_r} \right] \quad (20)$$

$$S = -R \left[\frac{dG_r}{dT_r} \right] \quad (21)$$

$$V = \frac{RT_B}{P_B} \left[\frac{dG_r}{dP_r} \right] \quad (22)$$

B. Water/Ammonia Mixture

The liquid mixture Gibbs function of ammonia water is given by the ideal solution mixing relationship plus the excess energy of Gibbs G_E . This energy, whose relation is proposed by Xu and Yogi Goswami, is limited to three factors, takes into account the deviation of the ideal behavior of solution (the liquid solution does not behave like an ideal solution) [19].

Enthalpy, entropy and excess volume are given by

$$G_r^E = x(1-x) \left[F_1 + F_2(2x-1) + F_3(2x-1)^2 \right] \quad (23)$$

Where

$$F_1 = E_1 + E_2 P_r + (E_3 + E_4 P_r) T_r + \frac{E_5}{T_r} + \frac{E_7}{T_r^2} \quad (24)$$

$$F_2 = E_7 + E_8 P_r + (E_9 + E_{10} P_r) T_r + \frac{E_{11}}{T_r} + \frac{E_{12}}{T_r^2} \quad (25)$$

$$F_3 = E_{13} + E_{14} P_r + \frac{E_{15}}{T_r} + \frac{E_{16}}{T_r^2} \quad (26)$$

The excess enthalpy; entropy and volume are given by:

$$H^E = -RT_B T_r^2 \left[\frac{d \left(\frac{G_r^E}{T_r} \right)}{dT_r} \right] \quad (27)$$

$$S^E = -R \left[\frac{dG_r^E}{dT_r} \right] \quad (28)$$

$$V^E = \frac{RT_B}{P_B} \left[\frac{dG_r^E}{dP_r} \right] \quad (29)$$

Therefore, the enthalpy, entropy and molar volume of the NH₃-H₂O liquid mixture becomes

$$H_m^L = xH_{NH_3}^L + (1-x)H_{H_2O}^L + H^E \quad (30)$$

$$V_m^g = yV_{NH_3}^g + (1-y)V_{H_2O}^g \quad (31)$$

$$V_m^L = xV_{NH_3}^L + (1-x)V_{H_2O}^L + V^E \quad (32)$$

where

$$S^{me} = -R \left[x \ln x + (1-x) \ln(1-x) \right] \quad (33)$$

The solution in the vapor phase was considered as an ideal solution [20].

This hypothesis is based on the absence of the excess Gibbs energy G^E . The enthalpy, entropy and molar volume of the $\text{NH}_3/\text{H}_2\text{O}$ vapor mixture are calculated by:

$$H_m^g = yH_{\text{NH}_3}^g + (1-y)H_{\text{H}_2\text{O}}^g \quad (34)$$

$$S_m^g = yS_{\text{NH}_3}^g + (1-y)S_{\text{H}_2\text{O}}^g + S^{mg} \quad (35)$$

$$V_m^g = yV_{\text{NH}_3}^g + (1-y)V_{\text{H}_2\text{O}}^g \quad (36)$$

where

$$S^{mg} = -R[y \ln y + (1-y) \ln(1-y)] \quad (37)$$

Table1: Water/ammonia mixture parameter

	<i>Ammonia</i>	<i>water</i>		<i>Mixture</i>
A_1	$3.971423 \cdot 10^{-2}$	$2.748796 \cdot 10^{-2}$	E1	-41.733398
A_2	$-1.790557 \cdot 10^{-5}$	$-1.01665 \cdot 10^{-5}$	E2	0.02414
A_3	$-1.308905 \cdot 10^{-2}$	$-4.452025 \cdot 10^{-3}$	E3	6.702285
A_4	$3.752836 \cdot 10^{-3}$	$8.389246 \cdot 10^{-4}$	E4	-0.011475
B_1	$1.634519 \cdot 10^1$	$1.214557 \cdot 10^1$	E5	63.608967
B_2	-6.508119	-1.898065	E6	-62.490768
B_3	1.448937	$2.911966 \cdot 10^{-1}$	E7	1.761064
C_1	$-1.049377 \cdot 10^{-2}$	$2.136131 \cdot 10^{-2}$	E8	0.008626
C_2	-8.288224	$-3.169291 \cdot 10^1$	E9	0.387983
C_3	$-6.647257 \cdot 10^2$	$-4.634611 \cdot 10^4$	E10	0.004772
C_4	$-3.045352 \cdot 10^3$	0	E11	-4.648107
D_1	3.673647	4.019170	E12	0.836376
D_2	$9.989629 \cdot 10^{-2}$	$-5.175550 \cdot 10^{-2}$	E13	-3.553637
D_3	$3.617622 \cdot 10^{-2}$	$1.951939 \cdot 10^{-2}$	E14	0.000904
$H_{r,0}^l$	4.878573	21.821141	E15	24.361723
$H_{r,0}^g$	26.468879	60.965058	E16	-20.736547
$S_{r,0}^l$	1.644773	5.733498		
$S_{r,0}^g$	8.339026	13.453430		
$T_{r,0}$	3.2252	5.0705		
$P_{r,0}$	2	3		

C. Vapor/liquid equilibrium properties

Patek&Klomfar (1995) presented a set of equations describing the vapor/liquid equilibrium properties of the ammonia-water mixture necessary for absorption cycle design. These equations are as an example of fast approximation functions, because they avoid iterative calculations. [21]

The bubble point temperature is calculated with Equation (30). The parameters needed for this calculation are given in Table 4.

$$T(P, x) = T_0 \sum_i a_i (1-x)^{m_i} \left[\ln \left(\frac{P_0}{P} \right) \right]^{n_i} \quad (38)$$

The dew point temperature is calculated from Equation (31). The parameters used in this equation are reported in Table 5.

$$T(P, y) = T_0 \sum_i a_i (1-y)^{m_i/4} \left[\ln \left(\frac{P_0}{P} \right) \right]^{n_i} \quad (39)$$

The vapor phase composition is calculated using Equation (32) and the parameters are given in Table 6.

$$y(P, x) = 1 - \exp \left(\ln(1-x) \sum_i a_i \left[\ln \left(\frac{P_0}{P} \right) \right]^{m_i} x^{n_i/3} \right) \quad (40)$$

Table 2: Parameters of Equation (38)

i	m_i	n_i	a_i	i	m_i	n_i	a_i
1	0	0	$+0.322302 \cdot 10^1$	8	1	2	$+0.106154 \cdot 10^{-1}$
2	0	1	-0.384206	9	2	3	$-0.533589 \cdot 10^{-3}$
3	0	2	$+0.460965 \cdot 10^{-1}$	10	4	0	$+0.785041 \cdot 10^1$
4	0	3	$-0.378945 \cdot 10^{-2}$	11	5	0	$-0.115941 \cdot 10^2$
5	0	4	$+0.135610 \cdot 10^{-3}$	12	5	1	$-0.523150 \cdot 10^{-1}$
6	1	0	+0.487755	13	6	0	$+0.489596 \cdot 10^1$
7	1	1	-0.120108	14	13	1	$+0.421059 \cdot 10^{-1}$
$T_0 = 100 \text{ K}; P_0 = 20 \text{ bar}$							

Table 3: Parameters of Equation (39)

i	m_i	n_i	a_i	i	m_i	n_i	a_i
1	0	0	$+1.98022017 \cdot 10^1$	8	3	2	$-3.42198402 \cdot 10^{-3}$
2	0	1	$-1.18092669 \cdot 10^1$	9	4	3	$+1.19403127 \cdot 10^{-4}$
3	0	6	$+2.77479980 \cdot 10^1$	10	5	4	$-2.45413777 \cdot 10^{-4}$
4	0	7	$-2.88634277 \cdot 10^1$	11	6	5	$+2.91591865 \cdot 10^{-4}$
5	1	0	$-5.91616608 \cdot 10^1$	12	7	6	$-1.84782290 \cdot 10^{-4}$
6	2	1	$+5.78091305 \cdot 10^2$	13	7	7	$+2.38419434 \cdot 10^1$
7	2	2	-6.21736743	14	8	7	$+4.80310617 \cdot 10^{-3}$
$P_0 = 20 \text{ bar}$							

Table 4: Parameters of Equation (34)

i	m _i	n _i	a _i	i	m _i	n _i	a _i
1	0	0	+0.324004·10 ¹	10	3	0	-0.201780·10 ²
2	0	1	-0.395920	11	3	1	+0.110834·10 ¹
3	0	2	+0.435624·10 ⁻¹	12	4	0	+0.145399·10 ²
4	0	3	-0.218943·10 ⁻²	13	4	2	+0.644312
5	1	0	-0.143526·10 ¹	14	5	0	-0.221246·10 ¹
6	1	1	+0.105256·10 ¹	15	5	2	-0.756266
7	1	2	-0.719281·10 ⁻¹	16	6	0	-0.135529·10 ¹
8	2	0	+0.122362·10 ²	17	7	2	+0.183541
9	2	1	-0.224368·10 ¹				
$T_0 = 100 \text{ K}; P_0 = 20 \text{ bar}$							

VII. CHILLER SIMULATION

The proposed absorption refrigeration machine will be installed in a storage cold room of 45m³, illustrated in fig.3, destined for conserving approximately 6 tons of fruits.

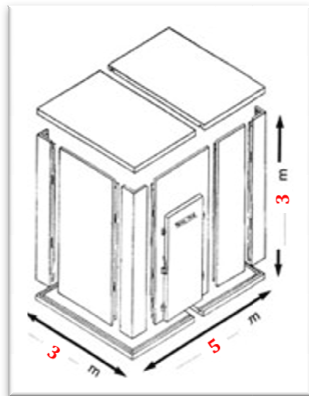


Figure 3: Cold room

A previous study of the storage cold room was elaborated in the condition of the south of Tunisia. The simulation of this cold room leads to an estimation of the frigorific power about 13 Kw. This thermal power is ensured by the evaporator of the absorption chiller.

A numerical simulation of the absorption machine was carried out using Matlab software version R2013a 8.1.0.604. The program were established using some hypothesis and operation conditions.

A. Hypothesis

In order to derive a mathematical model, the following key assumptions were made[2]:

- Steady state operation.

- Negligible pressure drop and heat loss in process units.

- The pump work is supposed isentropic.

- The expansion valves are isenthalpic

- The heat exchangers are supposed adiabatic [22]

- The condenser and absorber output liquid is assumed to be 4°C subcooled.

- The refrigerant leaving the condenser is assumed to be saturated liquid.

- The refrigerant leaving the evaporator is assumed to be saturated gas.

- The refrigerant vapor leaving the generator is superheated.

- The weak solution leaves the absorber is saturated liquid at equilibrium.

- The strong solution leaving the generator is in equilibrium at its respective temperature and pressure.

B. Operating conditions

The studied installation is a refrigeration system. The outlet evaporator temperature is set at 2°C and the maximum temperature in the generator is 120°C.

The condenser and the absorber with a temperature reaching 50°C; are cooled either by ambient air at an average temperature of 35°C or water at 25°C.

In comparison with the cooling medium, the end-of-condensation and absorption temperatures are assumed to be higher by 12 to 15°C with air cooling and 5°C with water cooling.

The vapor refrigerant purity of the generator outlet is between 95 and 100%. The condensation pressure, PC, is that of the saturated refrigerant.

The evaporation pressure varies between an upper and a lower limit. The upper limit corresponds to the saturated liquid pressure at the evaporator outlet temperature and to a molar composition equal to the purity of the refrigerant; above this value, the refrigerant won't evaporate. The lower limit corresponds to the liquid saturation pressure at an absorber temperature and to a poor solution molar composition; below this limit the refrigerant vapor cannot be absorbed by the poor solution. In this pressure range.

C. Thermodynamic Diagram

The conventional operation of absorption machines with different state changes uses two types of diagram:

a. Merkel diagram

Its Merkel's diagram that allow doing a full study of the absorption cycle, as it provides the heat balances of the various system components by direct reading of enthalpy differences. As shown in fig, the x-axis is dedicated to molar fraction and the y-axis to the enthalpy.

At the lower part of the diagram, networks of isobars and isotherms, as well as curves of vapor-liquid

equilibrium at equal concentration. At the upper part, a reference curves helps to establish the characteristics of the vapor phase. [20]

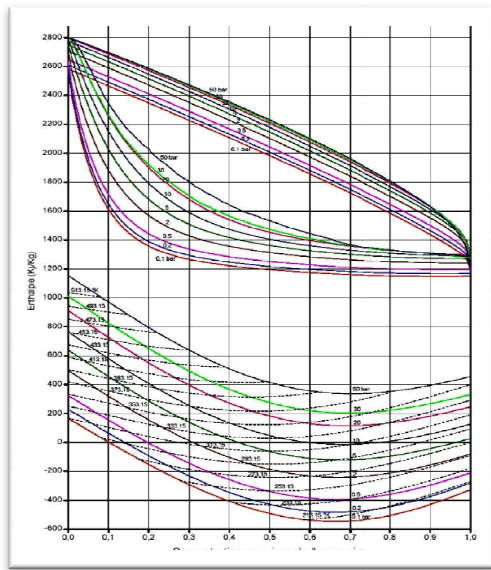


Figure 4 : Merkel diagram of NH₃/H₂O mixture

b. Oldham digram

It's the most convenient diagram used for the absorption system study. As shown in fig.5, the x-axis is scaled in $(1/T)$ and the y-axis dedicated to $(\log P)$. In this system of coordinates, straight lines represent curves of binary system balance in the vapor as well as in the liquid phase. Pure ammonia is represented with the straight line with 100% of concentration, and the one with 0% of concentration correspond to vapor-liquid equilibrium of pure water[23].

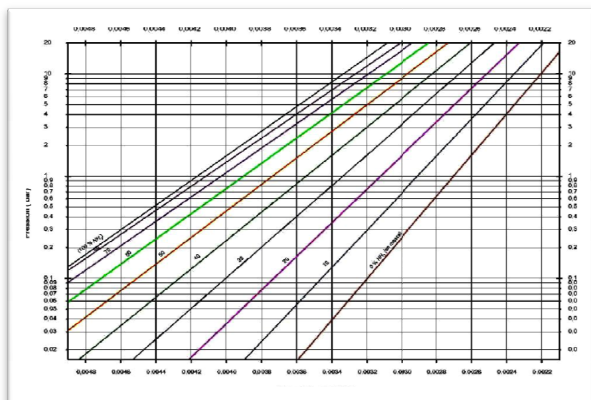


Figure 5: Oldham diagram of NH₃/H₂O mixture

The obtained numerical code calculates the thermodynamics properties of ammonia-water mixture at different points and states of the machine. Figure 6 and 7 shows the liquid – vapor equilibrium at the two working pressures of the machine as well as for the mass fraction and flow rates which will be shown in the following tables.

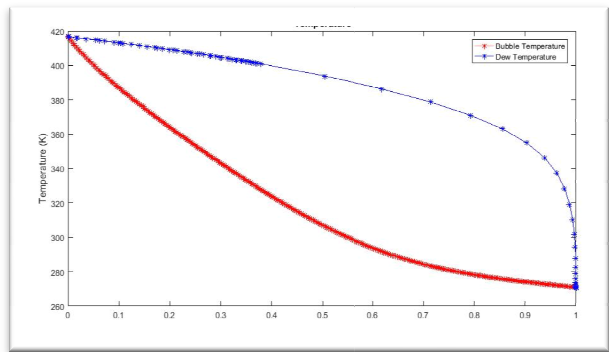


Figure 6: Low-pressure equilibrium

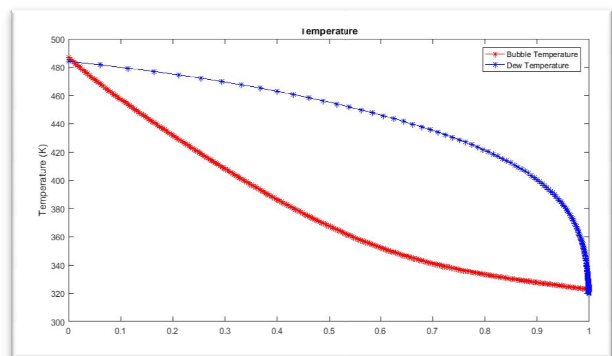


Figure 7: High-pressure equilibrium

Table5: Simulation Result at different point of the

Point	T (°C)	P (bar)	x
1	120	20.19	0.99
2	45	20.19	0.99
3	5	4	0.99
4	2	4	0.99
5	45	4	0.4
6	46	20.19	0.4
7	107	20.19	0.4
8	120	20.19	0.36
9	87	20.19	0.36
10	57	4	0.36

cycle

Table 6: Thermal power and COP

Thermal power (kW)	
Q _g	24.37
Q _a	28.25
Q _e	12.95
Q _c	15.92
Performance coefficient	
COP	0.53
COP _c	1.01
Flow rats (Kg/s)	
\dot{m}	0.0123
\dot{p}	0.2002
\dot{r}	0.2125
ϵ	0.8

VIII. RESULTS

To achieve the energetic study of a storage cold room destined to preserve fruits in the region, we proceed on two steps; the first one consists on the modelization of the cold room itself to predict the frigorific power required. An absorption refrigeration chiller working with NH₃/H₂O chiller ensures this power. The second step of this project is dedicated to the machine's analyse.

Simulation of ammonia-water machine leads to a coefficient of performance of about 0.5 which is an acceptable value since this 'kind of machines' are driven by heat energy and can even work with low grade heat such as solar energy or thermal waste. This alternative makes the study very interesting. Feeding the refrigeration machine with solar energy consists the following steps of this project.

The thermodynamic cycle of the proposed machine is illustrated in fig.8, it shows that the thermal compression is due to the absorption of ammonia by water to obtain a solution of 40% in NH₃ and the desorption leading to a solution of 36% in NH₃.

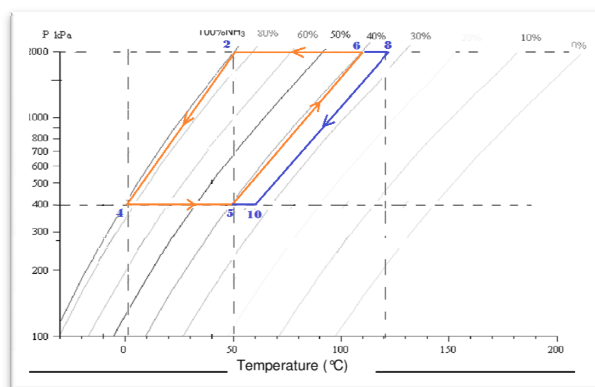


Figure 8: Simulation illustration in Oldham diagram

IX. CONCLUSION

An absorption refrigeration machine is simulated and studied to ensure the frigorific power required for a storage cold room destined for preserving foods in the south of Tunisia.

The actual basic machine has a COP of 0.53, an interesting value when considering that the proposed machine will be driven by solar energy, which its potential is important in the south of Tunisia. This study must be completed by an economic analysis of the solar plant associated with the chiller.

REFERENCES

[1] **Rabah Gomri**; "Second law comparison of single effect and double effect vapour absorption refrigeration systems" Energy Conversion and Management; Vol 50, 2009, pp 1279–1287.

[2] **Maria S. Mazzei, Miguel C. Mussati, Sergio F. Mussati** "NLP model-based optimal design of LiBr/H₂O absorption refrigeration systems" International Journal of Refrigeration; Vol 38, 2014, pp 58-70.

[3] **Pongsid Sriksirin, Satha Aphornratana, Supachart Chungpaibulpatana**, "A review of absorption refrigeration technologies" Renewable and Sustainable Energy Reviews, Vol 5, 2001, pp 343–372.

[4] **André Aleixo Manzela, Sérgio Morais Hanriot, Luben Cabezas-Gómez, José Ricardo Sodré**, "Using engine exhaust gas as energy source for an absorption refrigeration system", Applied Energy, Vol 87, 2010, pp 1141–1148.

[5] **N. Chekir, Kh. Mejri, A. Bellagi**, "Simulation of an absorption chiller operating with alkane mixtures", International Journal of Refrigeration, Vol 29, 2006, pp 469-475.

[6] **Anas Farraj, Mohammad Abu Mallouh, Abdul-Rahim Kalendarc, Abed Al-Rzaq Al-Shqirated and Mahmoud Hammad**, "Experimental Study of Solar Powered Air Conditioning Unit Using Drop – In Hydro Carbon Mixture to Replace R-22", Jordan Journal of Mechanical and Industrial Engineering, Vol 6, 2012, pp 63-70.

[7] **Bilal A. Akash, Salem A. Said**, "Assessment of LPG as a possible alternative to R-12 in domestic refrigerators", Energy Conversion and Management, Vol 44, 2003, pp 381–388.

[8] **Akhilesh Arora, S.C. Kaushik**, "Theoretical analysis of a vapour compression refrigeration system with R502, R404A and R507A, International Journal of refrigeration, Vol 31, 2008, pp 998–1005.

[9] **Filippo de Rossi, Rita Mastrullo and Pietro Mazzei**, "Energetic and thermodynamic comparison of R12 and R1 as vapour compression refrigeration working fluids"; International Journal of Refrigeration, 1993, Vol 16.

[10] **Basant K. Agrawal, Munawar N. Karimi**, "Thermodynamic performance assessment of a novel waste heat based triple effect refrigeration cycle, International Journal of refrigeration, Vol 35, 2012, 1647-1656.

[11] **Pongsid Sriksirin, Satha Aphornratana, Supachart Chungpaibulpatana**, "A review of absorption refrigeration technologies", Renewable and Sustainable Energy Reviews, Vol 5, 2001, pp 343-372.

[12] **Kh. Mejri, A. Bellagi**, "Modelling of the thermodynamic properties of the water–ammonia mixture by three different approaches" International Journal of Refrigeration, Vol 29, 2006, pp 211–218.

[13] **Dongsoo Jung, Chong-Bo Kim, Kilhong Song, Byoungjin Park**, "Testing of propane/isobutane mixture in domestic refrigerators", International Journal of Refrigeration Vol 23, 2000, pp 517-527

[14] **Berhane H. Gebreslassie, Eckhard A. Groll, Suresh V. Garimella**, "Multi-objective optimization of sustainable single-effect water/Lithium Bromide absorption cycle, Renewable Energy, Vol 46, 2012, pp 100–110.

[15] **Mohamed Lamine CHOUGUI**, «Simulation et étude comparée de cycle à absorption (LiBr/H₂O) à usage de froid. Cas de l'unité de production de détergent Henkel ». Master, 2010, Mentouri University CONSTANTINE.

[16] **Gearoid FOLEY, Robert DE VAULT and Richard SWEETSER**, "The Future Of Absorption Technology in America: A Critical Look at the impact Of BCHP and Innovation", Advanced Building System, 2000, Conference

[17] **André Aleixo Manzela, Sérgio Morais Hanriot, Luben Cabezas-Gómez, José Ricardo Sodré**, "Using engine exhaust gas as energy source for an absorption refrigeration system" Applied Energy, Vol 87, 2010, pp 1141-1148

[18] **Mohamed Hachemi Chibeni**, «Contribution à l'étude du dessalement solaire de l'eau de mer et des pompes à chaleur à sorption », University habilitation, Gabes University, Tunisia 2012.

[19] **HADJ Imad and BENSIDHOUM Abderkader**, « Contribution à l'amélioration des performances des installations à réfrigération solaire à absorption », Master,

Technology Faculty, Aboubakr BELKAID University, TLEMCEM.

- [20] **Sahraoui KHERRIS, Mohammed MAKHLOUF, Djallel ZEBBAR et Omar SEBBANE**, “ Contribution study of thermodynamics properties of the ammonia-water mixtures“, Sciences and Technologies Institute, Tissemsilt University, ALGERIA.
- [21] **Pedro Dinis Gaspar**, Handbook of Research on Advances and Applications in Refrigeration Systems and Technologies.p46-p48, University of Beira Interior, Portugal.
- [22] **NIHEL CHEKIR**, “Modelisation et dimensionnement d’une machine frigorifique a absorption fonctionnant avec des melanges d’hydrocarbure saturés », 2007, THESIS.
- [23] **Mohamed H, BEN BRAHIM A**, “Modeling of the absorption phase of a cycle with solar absorption using the couple $\text{NH}_3\text{-H}_2\text{O}$ for in-sight energy storage”, International Journal of Hydrogen Energy, 2016.